



Published in final edited form as:

*J Orthop Res.* 2017 January ; 35(1): 193–199. doi:10.1002/jor.23273.

## Novel In Vivo Mouse Model of Implant Related Spine Infection

Eric E. M. D. Dworsky<sup>1</sup>, Vishal V. H. Hegde<sup>1</sup>, Amanda A. H. L. Loftin<sup>1</sup>, Sherif S. R. Richman<sup>1</sup>, Yan Y. H. Hu<sup>1</sup>, Elizabeth E. L. Lord<sup>1</sup>, Kevin Patrick K. P. F. Francis<sup>1</sup>, Lloyd L. S. M. Miller<sup>2</sup>, Jeff J. C. W. Wang<sup>3</sup>, Anthony A. S. Scaduto<sup>1</sup>, and Nicholas Matthew N. M. B. Bernthal<sup>1</sup>

<sup>1</sup>Department of Orthopaedic Surgery, David Geffen School of Medicine at University of California Los Angeles (UCLA), Santa Monica 90404 California <sup>2</sup>Department of Dermatology, Johns Hopkins School of Medicine, Baltimore 21231 Maryland <sup>3</sup>Department of Orthopaedic Surgery, Keck School of Medicine at University of Southern California (USC), Los Angeles 90017 California

### Abstract

Post-operative spine infections are a challenge, as hardware must often be retained to prevent destabilization of the spine, and bacteria form biofilm on implants, rendering them inaccessible to antibiotic therapy, and immune cells. A model of posterior-approach spinal surgery was created in which a stainless steel k-wire was transfixed into the L4 spinous process of 12-week-old C57BL/six mice. Mice were then randomized to receive either one of three concentrations ( $1 \times 10^2$ ,  $1 \times 10^3$ , and  $1 \times 10^4$  colony forming units (CFU)) of a bioluminescent strain of *Staphylococcus aureus* or normal saline at surgery. The mice were then longitudinally imaged for bacterial bioluminescence to quantify infection. The  $1 \times 10^2$  CFU group had a decrease in signal down to control levels by POD 25, while the  $1 \times 10^3$  and  $1 \times 10^4$  CFU groups maintained a 10-fold higher signal through POD 35. Bacteria were then harvested from the pin and surrounding tissue for confirmatory CFU counts. All mice in the  $1 \times 10^4$  CFU group experienced wound breakdown, while no mice in the other groups had this complication. Once an optimal bacterial concentration was determined, mice expressing enhanced green fluorescent protein in their myeloid cells (Lys-EGFP) were utilized to contemporaneously quantify bacterial burden, and immune response. Neutrophil fluorescence peaked for both groups on POD 3, and then declined. The infected group continued to have a response above the control group through POD 35. This study, establishes a noninvasive in vivo mouse model of spine implant infection that can quantify bacterial burden and host inflammation longitudinally in real time without requiring animal sacrifice.

---

Correspondence to: Nicholas M. Bernthal (T: +424-259-9860; F: +424-259-6598; nbernth@mednet.ucla.edu).

### AUTHORS' CONTRIBUTIONS

Eric Dworsky was the primary author of the manuscript, helped develop the research questions behind the study, and performed the statistical analysis. Vishal Hegde was the secondary author of the manuscript, helped develop the research questions behind the study, and provided critical revisions of the paper. Amanda Loftin, Sherif Richman, Yan Hu, and Elizabeth Lord helped carry out the experiments, collect data, and draft the manuscript. Kevin Francis refined the research questions, helped write the manuscript, and provided critical revisions of the paper. Nicholas Bernthal, Anthony Scaduto, Jeff Wang, and Lloyd Miller helped write the manuscript, develop the research questions, and refine the experimental techniques used. All authors have read and approved the submitted manuscript.

## Keywords

spine; implant infection; *Staphylococcus*; bioluminescence

Infection after spine surgery is a devastating complication for both patients and their orthopedic surgeons. Despite advances in perioperative antibiotic management and aseptic surgical technique, post-operative infection still occurs in approximately 3–8% of elective spine surgery.<sup>1–5</sup> The rate of infection can be even higher for multilevel or revision surgeries, with one study suggesting infection rates as high as 65%.<sup>6</sup> Spinal implant infections are disastrous for patients, surgeons, and our health system as a whole. Despite multiple hospitalizations, repeat surgeries and long courses of antibiotics, these infections often result in neurological compromise, disability and even potentially death. Managing these infections can be extremely expensive, with the treatment of a single implant associated spinal infection costing upwards of \$900,000.<sup>7</sup>

The majority of spinal implant infections are caused by *Staphylococcus aureus*,<sup>8–11</sup> although recent literature has identified *Staphylococcus epidermidis* and *Propionibacterium acnes* to be secondary pathogens.<sup>12,13</sup> These bacteria can seed the hardware either during surgery, or later by local, or hematogenous spread. Once bacteria seed the implant, they form a protective biofilm surface rendering them insusceptible to antibiotic therapy or immune cells. Unlike in other areas of orthopaedics, spinal infections are unique in that the infected implant often cannot be removed surgically without causing potential destabilization of the spine.<sup>12</sup>

Given the absence of a surgical “explantation” option, novel therapies and techniques are being developed to prevent, and treat spine implant infections. Unfortunately, these therapies often do not progress beyond the hypothetical, as there are no efficient, accurate, and available animal models to assess safety and efficacy. Current animal models of spine infection require large numbers of animals, as all data points are invasive (colony counting, histology, culture) and require euthanasia of the animal.<sup>14–16</sup> These models are therefore, extremely expensive and inefficient, providing a single data point per animal.

Previous work outside of the spine has established the accuracy, efficiency and value of noninvasive in vivo imaging, especially optical imaging, to replace euthanasia-based models to study infection.<sup>17</sup> This technology quantifies bacterial burden without sacrificing animals and allows real-time, longitudinal study in a humane, accurate, and efficient manner. Previous studies, have demonstrated that in vivo bioluminescence highly correlates with the numbers of CFUs adherent to implants.<sup>18</sup> This capacity to watch infection over time, and in response to alterations in the system (antibiotics, implant coatings, immune modulation), has led to a better understanding of the pathophysiology of implant infection, the effectiveness of antibiotic therapy, and the development of novel antimicrobial therapies.<sup>17–19</sup> Additionally, advances in murine genetic engineering now provide a plethora of options for fluorescent labeling of host cells. Given that bioluminescence is the emission of high-energy light (490 nm) through an enzymatic process within the organism itself, indicating live, actively metabolizing bacteria, and fluorescence is a process in which energy from an external light source is absorbed by a substance and re-emitted at a lower energy wavelength

(~515–575 nm), these distinct processes can be co-registered simultaneously without overlap or interference.<sup>20</sup> This allows contemporaneous imaging of the infection (bioluminescence) and the host immune response (fluorescence), such that the interplay between infection and host can begin to be understood in vivo, and in real time.

Given the availability of these powerful tools for real time imaging, we aim to develop a model of postoperative spinal implant infection by asking two major questions. First, what is the optimal bacterial load of bioluminescent *S. aureus* required to develop a chronic, low-grade infection that would allow longitudinal, non-invasive study, without exposing the animal to local toxicity? Second, can the model be reproduced in mice with fluorescent-labeled neutrophils (LysEGFP) as a proof of principle to confirm its use for simultaneous evaluation of the immune response to infection? We therefore, hypothesize that an inoculum of between  $1 \times 10^2$  and  $1 \times 10^4$  CFUs could be used to establish a spine implant infection that could be longitudinally followed and implemented in genetically modified mice to allow contemporaneous quantification of bacterial burden, and immune response.<sup>17–19</sup> This model would be an inexpensive, rapid, and accurate in vivo tool to test potential therapeutics and treatment strategies for spinal implant infections prior to their application in larger animal models, and clinical trials.

## MATERIALS AND METHODS

### Ethics Statement

All animals were handled in strict accordance with good animal practice as defined in the federal regulations set forth in the Animal Welfare Act (AWA), the 1996 Guide for the Care and Use of Laboratory Animals, PHS Policy for the Humane Care and Use of Laboratory Animals, as well as UCLA's policies, and procedures as set forth in the UCLA Animal Care and Use Training Manual. All animal work was approved by the UCLA Chancellor's Animal Research Committee (ARC# 2012-104-03J).

### *S. aureus* Bioluminescent Strain

*S. aureus* Xen36, (PerkinElmer, Hopkinton, MA) is a bioluminescent derivative of the parental strain *S. aureus* ATCC 49525 (Wright), a clinical isolate from a bacteremia patient. *S. aureus* Xen36 possesses a Gram-positive optimized *lux-ABCDE* operon stably integrated into a large native plasmid.<sup>21</sup> This allows the bacteria to produce a blue-green light with a maximal emission wavelength of approximately 490 nm, which is only produced by live metabolically active bacteria. It has been previously shown to be the optimal *S. aureus* strain for use in such experiments due to the strength and consistency of its bioluminescent signal.<sup>17</sup>

### Preparation of *S. aureus* for Inoculation

*S. aureus* Xen36 has a kanamycin resistance selection marker on its *lux* operon, allowing it to be isolated from potentially contaminating background strains during culture. Thus, 200 µg/ml kanamycin (Sigma–Aldrich) was supplemented to all cultures to ensure consistency. *S. aureus* was streaked onto tryptic soy agar plates (tryptic soy broth [TSB] plus 1.5% bacto agar, BD Biosciences) and grown at 37° C overnight. Single colonies of *S. aureus* were then

cultured in TSB and again grown overnight at 37°C in a shaking incubator (240 rpm) (MaxQ 4,450, Thermo). Mid-logarithmic phase bacteria were obtained after a 2 h subculture of a 1:50 dilution of the overnight culture. Bacterial cells were pelleted, re-suspended, and washed three times in phosphate buffered saline (PBS). Bacterial inocula ( $1 \times 10^2$ ,  $1 \times 10^3$ ,  $1 \times 10^4$  CFUs in 2 ml PBS) were approximated by measuring the absorbance at 600 nm (A600, Biomate 3 [Thermo]).

## Mice

Twelve-week-old male C57BL/six wildtype mice were used (Jackson Laboratories, Bar Harbor, ME) in the bacterial optimization experiment. In the latter experiments co-registering bacterial burden and immune response, 2-week-old male LysEGFP mice were used. LysEGFP mice are genetically engineered on a C57BL/6 background with green-fluorescent myeloid cells (mostly neutrophils) via a “knock-in” of enhanced green fluorescence protein (EGFP) into the lysozyme M gene.<sup>22,23</sup> Animals were kept at four mice per cage in standard cages with a 12 h light and dark cycle. They were fed a standard pellet diet with free access to bottled water. Assessments were carried out daily by veterinary staff to ensure the well being of all animals throughout the experiment.

## Mouse Surgical Procedures

Survival surgery was performed in which a custom, “L-shaped” surgical-grade 0.1 mm diameter stainless steel implant (Modern Grinding, Port Washington, WI) was press-fit into the L4 spinous process (Fig. 1). Mice were anesthetized via inhalation isoflurane (2%). The level of the L4 spinous process was approximated by the position of the knee with the hip maximally flexed. A 2 cm midline incision was then made and carried down through fascia, and muscle to the osseous spine. The dissection was directed laterally along the right side of the spinous processes, visualizing the lateral aspect of the process, and developing a pocket for the implant. A 25-gauge needle was oriented perpendicular to the L4 spinous process and, rotating the needle between forefinger and thumb, the needle was inserted through the spinous process. The implant was then loaded into a needle driver and inserted into the spinous process defect created by the needle. With the short arm of the implant in the spine, the long arm was placed longitudinally along the spine heading cranially. The wound was prepared for a closure with two 4/0 vicryl sutures. These sutures were placed but not tied to allow for expedient closure after inoculation and to restrict bacteria to the immediate area of the implant. An inoculation of  $1 \times 10^2$ ,  $1 \times 10^3$ , or  $1 \times 10^4$  CFUs of bioluminescent Xen36 *S. aureus* or sterile saline (control group) was pipetted onto the 90° bend of the implant. Deep sutures were tied and a running 4/0 vicryl was used to approximate the skin. Sustained release buprenorphine (2.5 mg/kg) (Zoo-Pharm, Fort Collins, CO) was administered subcutaneously every 72 h as analgesic for the duration of the experiment. Placement of the implant was confirmed with high resolution x-rays on POD 0 (Faxitron LX-60 DC-12 imaging system). All surgeries were performed on the same day using the same bacterial preparations.

### Quantification of *S. aureus* With In Vivo Bioluminescence Imaging

Mice were anesthetized via inhalation isoflurane (2%) and in vivo bioluminescence imaging was performed using an IVIS Lumina II (PerkinElmer).<sup>1-3</sup> Images were obtained on POD 0, 1, 3, 5, 7, 10, 14, 18, 21, 25, and 35. Data are presented via color scale overlaid on a grayscale photograph of mice and quantified as mean maximum flux (photons per second (s) per cm<sup>2</sup> per steradian (sr) [p/s/cm<sup>2</sup>/sr]) within a circular region of interest (16,103 pixels) using Living Image software (PerkinElmer).

### Validation of the Model With Bacterial CFU Counts

In order to validate the bioluminescence signal represented an accurate measure of bacterial burden, bacteria adherent to the implants and in surrounding soft tissue were quantified at POD 35. Bacteria were detached from the implant by sonication in 1 ml 0.3% Tween-80 in TSB for 10 min followed by vortexing for 5 min as previously described.<sup>18</sup> In addition, bacteria in the surrounding joint tissue were measured by homogenizing bone and joint tissue (Pro200H Series homogenizer; Pro Scientific). The number of bacterial CFU, that were adherent to the implant and in the joint tissue was determined by counting CFU after overnight culture of plates, and were expressed as total CFU harvested.

### Quantification of Neutrophil Recruitment With In Vivo Fluorescence Imaging

LysEGFP mice were used to contemporaneously measure neutrophil infiltration. After in vivo bioluminescence imaging, in vivo fluorescence imaging was performed using the IVIS Lumina II. EGFP-expressing neutrophils recruited to the operative site were visualized using the GFP filter for excitation (445–490 nm) and emission (515–575 nm) at an exposure time of 0.5 s.<sup>4-5</sup> Data are presented via color scale overlay on a grayscale photograph of mice and quantified as maximum radiant efficiency ([photons/s]/[μW/cm<sup>2</sup>]) within a circular region of interest (16103 pixels) using Living Image software.

### Statistical Analysis

Each group had six mice based on previous reports from our group showing that six animals/group was necessary to attain statistical significance at the  $p < 0.05$  level.<sup>17,18</sup> Data between two groups were compared by using a Student's *t*-test (one or two-tailed where indicated), while data between three or more groups were compared using a one-way ANOVA. All data are expressed as mean ± standard error of the mean (SEM). Values of  $p < 0.05$  were considered statistically significant.

## RESULTS

### In Vivo Bioluminescence of Different Inoculums During a Spinal Implant Infection and Corresponding CFU

All inocula ( $1 \times 10^2$ ,  $1 \times 10^3$ , or  $1 \times 10^4$  CFUs) had a concentration dependent increase in bioluminescent signal that peaked on post-operative day (POD) 10 ( $1.1 \times 10^6$ ,  $4.2 \times 10^6$ , and  $6.5 \times 10^6$  p/s/cm<sup>2</sup>/sr, respectively) (Fig. 2). In the  $1 \times 10^2$  group, the signal then decreased gradually and became statistically indistinguishable from the control group at POD 25, suggesting resolution of the infection ( $p = 0.53$ ). In contrast, the signal for the  $1 \times 10^3$  and 1

$\times 10^4$  CFU groups peaked at POD 10, but, maintained a 10-fold higher bioluminescence signal than uninfected control mice through day 35 ( $p < 0.05$ ), suggesting a successfully established implant infection. The accuracy of the non-invasive imaging was confirmed with CFU counts from the implant and surrounding joint tissue taken at POD 35 (Fig. 3). The average CFU from the implant were  $6 \times 10^0$ ,  $2.7 \times 10^2$ , and  $3.4 \times 10^2$  for the  $1 \times 10^2$ ,  $1 \times 10^3$ , and  $1 \times 10^4$  groups, respectively ( $p = 0.002$ ).

Clinically all mice in the  $1 \times 10^2$  and  $1 \times 10^3$  CFU groups recovered quickly from surgery and healed their surgical wounds. All six mice in the  $1 \times 10^4$  CFU groups, however, developed skin breakdown around the implant site, in one case with exposed hardware (Fig. 4). The average time until the appearance of wound breakdown was POD 5. Animals with skin breakdown were observed. The one mouse with exposed hardware was sacrificed on POD 14. This data, summed with the bioluminescence data above, suggests that  $1 \times 10^3$  CFUs is a sufficient inoculum to create a chronic implant infection yet, safe enough to avoid local wound breakdown.

### **In Vivo Neutrophil EGFP-Fluorescence Induced by *S. aureus* During a Post-Spinal Implant Infection**

Based on the results of the bioluminescence experiment, LysEGFP mice were inoculated with  $1 \times 10^3$  CFUs of *S. aureus* or a saline control, and in vivo bioluminescence and fluorescence imaging was performed coincidentally to measure the bacterial burden, and the degree of EGFP-neutrophil fluorescence in the infected post-operative spine for 35 days. As expected, bacterial burden was significantly higher for the infected group than the uninfected group throughout the 35 days ( $p < 0.05$ ) (Fig. 5). In terms of immune response, both groups had a progressive increase in fluorescent signal that peaked on POD 3 ( $3.5 \times 10^8$  and  $2.5 \times 10^8$  [photons/s]/[ $\mu\text{W}/\text{cm}^2$ ], respectively). Both groups then experienced a gradual decrease in signal, although the signal in the infected group remained significantly higher than the control group throughout the 35-day post-operative period ( $1.3 \times 10^8$  and  $8.4 \times 10^7$  [photons/s]/[ $\mu\text{W}/\text{cm}^2$ ], respectively) ( $p < 0.05$ ). This demonstrates that an infection was established, and resulted in an increased neutrophil-driven inflammatory response that persisted for 35 days after the surgical procedure.

## **DISCUSSION**

Infection after instrumented spine surgery is a catastrophic complication.<sup>1-5</sup> Unlike most other orthopedic implant infections, spine implant infections are unique in that the hardware is not typically removed to prevent destabilization of the spine. This makes treatment challenging, as bacteria adhere to the metal surface, forming biofilm that significantly blunts the efficacy of antibiotics, and the immune response.<sup>12</sup> Consequently, these infections can require extensive additional medical and surgical care which increases morbidity, and often results in poorer clinical outcomes.<sup>7</sup> To further our knowledge of these infections and advance our ability to prevent them, an accurate, efficient, humane animal model was needed to effectively test novel antimicrobial therapies, and better understand host immune response. To this end, we aimed to develop a mouse model of spine implant infection using noninvasive, contemporaneous in vivo bioluminescence, and fluorescence imaging.

In 1998, Guiboux et al. designed one of the first animal models of instrumented spine infection.<sup>15</sup> This model was utilized to investigate the effects of both instrumentation and perioperative antibiotics on infection following spine surgery. Since that time numerous other models have been developed, including a rat model by Ofluoglu et al. and rabbit model by Poelstra et al.<sup>14,24</sup> While each model presented advantages, all required invasive, ex vivo tissue analysis to evaluate results. This meant large cohorts of animals, inefficient study, and an inability to watch infection or host response over time. During this same period, models of infection have been established outside of the spine that have used non-invasive, real time in vivo optical imaging to replace static tissue study.<sup>17-19</sup> This capacity to watch infection longitudinally, and study the response of the bacteria to antibiotics, coatings, or immune modulation, has dramatically furthered our understanding of implant infection. Coupling these imaging modalities with host manipulation from genetic engineering allows simultaneous quantification of the infection (bioluminescence), and the host immune response (fluorescence) such that the interplay between infection and host can begin to be understood in vivo, and in real time. This study puts forth the first post-operative spine implant infection model in which both bacteria and host can be studied efficiently, accurately, and contemporaneously. Given that the wavelengths for bioluminescence (490 nm) and fluorescence (515–575 nm) are distinct, both can be measured simultaneously in the same mouse without crossover artifact.

The optimal concentration of Xen36 for the establishment of a chronic infection was found to be  $1 \times 10^3$  CFU. Lower dosing of bacteria was cleared by the host immune system and higher dosing caused wound breakdown. As this wound breakdown would not have differentiated between a deep implant infection and a superficial wound infection, the  $1 \times 10^4$  CFU inoculum was not deemed appropriate for this model. Consequently, we selected the  $1 \times 10^3$  CFU inoculum for study in the genetically-modified LysEGFP mice to show the persistent elevation of a neutrophil-driven immune response to the low grade infection over time. This finding serves as evidence of the power of the model, allowing contemporaneous study of host and bacteria in real time. Moreover, this model provides tremendous flexibility for modifications to be made, such as the inclusion of antibiotics and implant coatings, or adjustments to the host's immune status, enabling the development of more efficacious antimicrobials and/or immune modulators.

There are some limitations of this model. First, it is clear that this model is a considerable simplification of the steps involved in spinal implant surgery. Minimal bone was resected, the implant was placed unilaterally involving only the posterior elements of the spine, and all implants were stainless steel. Placement of implants bilaterally, and involvement of anterior elements of the spine such as the adjacent intervertebral discs may effect the interplay between host and bacteria in human spinal implant surgeries. In addition, other metals or materials used in human spine implant surgery may have different susceptibilities to bacterial infection. Another possible weakness is that braided vicryl suture was used for wound closure, which theoretically could be a nidus for bacteria to form biofilm. We believe this is not a significant concern given (i) previous studies done by our lab using three-dimensional imaging that demonstrated no bacterial burden in close proximity to the skin, (ii) the fact that CFU from the implant and peri-implant tissue correlate closely with the bioluminescent signal, and (iii) the bioluminescent signal is unilateral on the spine and

oriented in a longitudinal fashion, precisely how the implant is positioned along the spine.<sup>19</sup> This is compared to a suture-related infection which would have bioluminescence oriented horizontally, crossing the midline of the mouse. In addition, this study used only LysEGFP mice to assess immune response, which is reflective of only one portion of the host defense response. Myeloid cells are only present in the early immune response and other types of genetically modified mice, such as MacGreen mice, would be needed to monitor monocyte/macrophage lineages which are present later.<sup>25</sup> Yet, the aim of these experiments was to establish the murine model and develop an optimal inoculum for its use. Future study using this model can investigate the immune response in more detail using different strains of genetically engineered mice. Lastly, this model was also used only to study infections that were acquired during the surgical procedure and not against late infections, such as those that occur through hematogenous spread.

Despite these weaknesses, we believe this study successfully demonstrates a novel in vivo mouse model of spinal implant infection.  $1 \times 10^3$  CFU is the ideal inoculum of *S. aureus* Xen36 as it is sufficient to establish a sustained infection but not locally toxic enough to induce wound breakdown. This model could be used in the future to evaluate current strategies to combat implant related spine infection, including vancomycin powder, antibiotic loaded beads, and systemic antibiotic therapy, or to investigate new diagnostic and therapeutic modalities to help in the prevention of these devastating infections. In addition, this mouse model may also be used to analyze the mechanisms and pathways of the host immune response to implant related spine infection. With a plethora of anecdotal evidence driving surgical decision making today, we believe this model presents a powerful tool for a more scientific approach to the disastrous issue of spinal implant infections.

## Acknowledgments

Grant sponsor: Pediatric Orthopaedic Society of North America; Grant sponsor: National Center for Advancing Translational Sciences; Grant number: KL2TR000122; Grant sponsor: National Institutes of Health Clinical and Translational Science Institute; Grant sponsor: AO Foundation.

The authors would like to acknowledge the receipt of both the Pediatric Orthopaedic Society of North America Biomet Spine Grant and the National Institutes of Health Clinical and Translational Science Institute KL2 Grant as major funding sources for these experiments. Dr. Kevin P. Francis is employed by PerkinElmer, the manufacturer of the IVIS Lumina II imaging machine used in these experiments. Dr. Jeffrey Wang receives royalties from Biomet, Stryker, Seaspine, Aesculap, Osprey, Amedica, and Synthes; has investments in Bone Biologics, Amedica, Corespine, Expanding Ortho, VG Innovations, Pearldiver, Flexuspine, Fziomed, Benvenue, Promethean, Nexgen, Electrocore, and Surgitech; and receives fellowship funding from the AO foundation.

## References

1. Verdrengh M, Tarkowski A. Role of neutrophils in experimental septicemia and septic arthritis induced by *Staphylococcus aureus*. *Infect Immun*. 1997; 65:2517–2521. [PubMed: 9199413]
2. Fang A, Hu SS, Endres N, et al. Risk factors for infection after spinal surgery. *Spine*. 2005; 30:1460–1465. [PubMed: 15959380]
3. Levi AD, Dickman CA, Sonntag VK. Management of postoperative infections after spinal instrumentation. *J Neurosurg*. 1997; 86:975–980. [PubMed: 9171176]
4. Weinstein MA, McCabe JP, Cammisa FP. Postoperative spinal wound infection: a review of 2, 391 consecutive index procedures. *J Spinal Disord*. 2000; 13:422–426. [PubMed: 11052352]



5. Picada R, Winter RB, Lonstein JE, et al. Postoperative deep wound infection in adults after posterior lumbosacral spine fusion with instrumentation: incidence and management. *J Spinal Disord.* 2000; 13:42–45. [PubMed: 10710149]
6. Smith JS, Shaffrey CI, Sansur CA, et al. Rates of infection after spine surgery based on 108, 419 procedures: a report from the Scoliosis Research Society Morbidity and Mortality Committee. *Spine.* 2011; 36:556–563. [PubMed: 21192288]
7. Abbey DM, Turner DM, Warson JS, et al. Treatment of postoperative wound infections following spinal fusion with instrumentation. *J Spinal Disord.* 1995; 8:278–283. [PubMed: 8547767]
8. Silber JS, Anderson DG, Vaccaro AR, et al. Management of postprocedural discitis. *Spine J.* 2002; 2:279–287. [PubMed: 14589480]
9. Pappou IP, Papadopoulos EC, Sama AA, et al. Postoperative infections in interbody fusion for degenerative spinal disease. *Clin Orthop Relat Res.* 2006; 444:120–128. [PubMed: 16523136]
10. Sampredo MF, Huddleston PM, Piper KE, et al. A biofilm approach to detect bacteria on removed spinal implants. *Spine.* 2010; 35:1218–1224. [PubMed: 20445479]
11. Pull ter Gunne AF, Mohamed AS, Skolasky RL, et al. The presentation, incidence, etiology, and treatment of surgical site infections after spinal surgery. *Spine.* 2010; 35:1323–1328. [PubMed: 20150831]
12. Olsen MA, Mayfield J, Laurysen C, et al. Risk factors for surgical site infection in spinal surgery. *J Neurosurg.* 2003; 98:149–155. [PubMed: 12650399]
13. Nandyala SV, Schwend RM. Prevalence of intra-operative tissue bacterial contamination in posterior pediatric spinal deformity surgery. *Spine.* 2013; 38:E482–486. [PubMed: 23370682]
14. Ofluoglu EA, Zileli M, Aydin D, et al. Implant-related infection model in rat spine. *Arch Orthop Trauma Surg.* 2007; 127:391–396. [PubMed: 17522873]
15. Guiboux J-P, Ahlgren B, Patti JE, et al. The role of prophylactic antibiotics in spinal instrumentation: a rabbit model. *Spine.* 1998; 23:653. [PubMed: 9549786]
16. Stavrakis AI, Loftin AH, Lord EL, et al. Current animal models of postoperative spine infection and potential future advances. *Front Med.* 2015; 2:1–5.
17. Pribaz JR, Bernthal NM, Billi F, et al. Mouse model of chronic post-arthroplasty infection: noninvasive in vivo bioluminescence imaging to monitor bacterial burden for long-term study. *J Orthop Res.* 2011; 30:335–340. [PubMed: 21837686]
18. Bernthal NM, Stavrakis AI, Billi F, et al. A mouse model of post-arthroplasty staphylococcus aureus joint infection to evaluate in vivo the efficacy of antimicrobial implant coatings. *PLoS ONE.* 2010; 5:e12580–12611. [PubMed: 20830204]
19. Niska JA, Meganck JA, Pribaz JR, et al. Monitoring bacterial burden, inflammation, and bone damage longitudinally using optical and  $\mu$ CT imaging in an orthopaedic implant infection in mice. *PLoS ONE.* 2012; 7:e47397–47412. [PubMed: 23082163]
20. Bernthal NM, Pribaz JR, Stavrakis AI, et al. Protective role of IL-1 $\beta$  against post-arthroplasty Staphylococcus aureus infection. *J Orthop Res.* 2011; 29:1621–1626. [PubMed: 21445990]
21. Francis KP, Joh D, Bellinger-Kawahara C, et al. Monitoring bioluminescent Staphylococcus aureus infections in living mice using a novel luxABCDE construct. *Infect Immun.* 2000; 68:3594–3600. [PubMed: 10816517]
22. Kim M-H, Curry F-RE, Simon SI. Dynamics of neutrophil extravasation and vascular permeability are uncoupled during aseptic cutaneous wounding. *Am J Physiol Cell Physiol.* 2009; 296:C848–856. [PubMed: 19176758]
23. Kim M-H, Liu W, Borjesson DL, et al. Dynamics of neutrophil infiltration during cutaneous wound healing and infection using fluorescence imaging. *J Invest Dermatol.* 2008; 128:1812–1820. [PubMed: 18185533]
24. Poelstra KA, Berekzi NA, Grainger DW, et al. A novel spinal implant infection model in rabbits. *Spine.* 2000; 25:406. [PubMed: 10707383]
25. Sasmono RT, Williams E. Generation and characterization of MacGreen mice, the Cfs1r-EGFP transgenic mice. *Methods Mol Biol.* 2012; 844:157–176. [PubMed: 22262441]

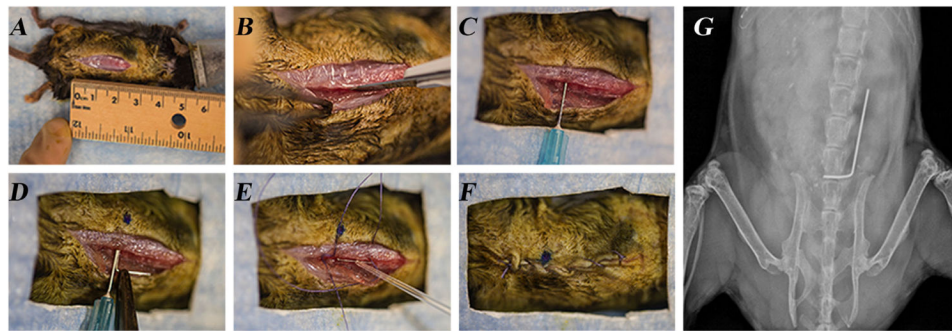


**Figure 1.**

Mouse surgical procedures. (A) A 2 cm midline incision was made in the skin overlying the spine. (B) The dissection was directed laterally along the L4 spinous process. (C) The L4 spinous process was manually reamed with a 25-gauge needle. (D) An orthopaedic-grade stainless steel K-wire (diameter 0.1 mm) was surgically placed into the L4 spinous process and placed lengthwise along the spine. (E) An inoculum of *S. aureus* Xen36 in a 0.2 ml volume was pipetted onto the implant. (F) The surgical site was closed with subcutaneous 4–0 Vicryl sutures. (G) A representative radiographic image demonstrating the placement of the implant in the L4 spinous process and lying lengthwise along the spine.

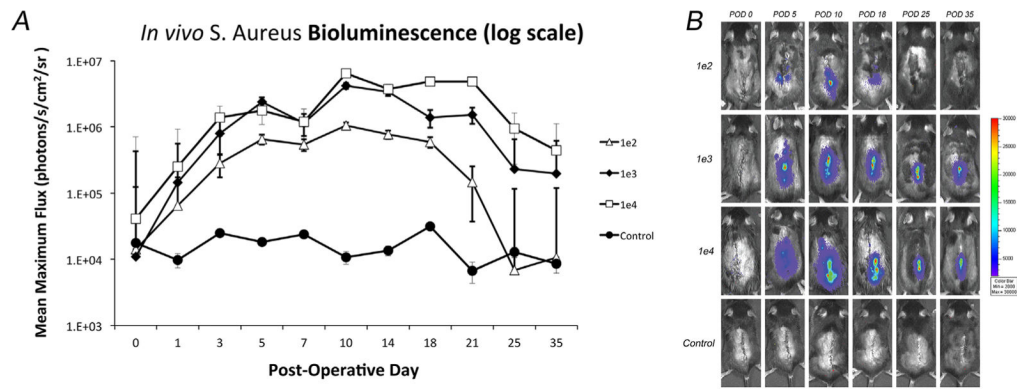


**Figure 2.**

Measurement of bacterial burden using in vivo bioluminescence. *S. aureus* possessing the bioluminescent construct in a stable plasmid (Xen36) in three inoculums ( $1 \times 10^2$ ,  $1 \times 10^3$ ,  $1 \times 10^4$  CFU) or no bacteria as a control ( $n=6$  mice per group) were inoculated into the L4 spinous process of mice in the presence of a stainless steel implant. (A) Bacterial counts as measured by in vivo *S. aureus* bioluminescence (mean maximum flux [photons/s/cm<sup>2</sup>/sr]  $\pm$  sem [logarithmic scale]). (B) Representative in vivo *S. aureus* bioluminescence on a color scale overlaid on top of a grayscale image of mice.

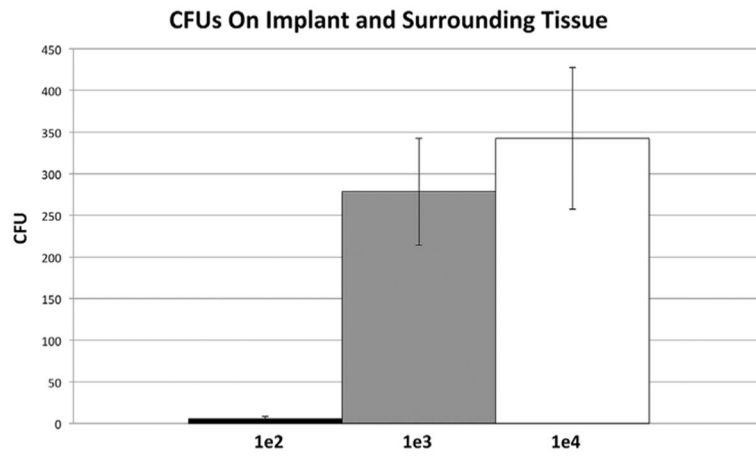


**Figure 3.** Confirmation of bacterial burden using CFU counts. At POD 35, mice were sacrificed, pins were sonicated, tissue was homogenized, and bacteria was cultured and counted.

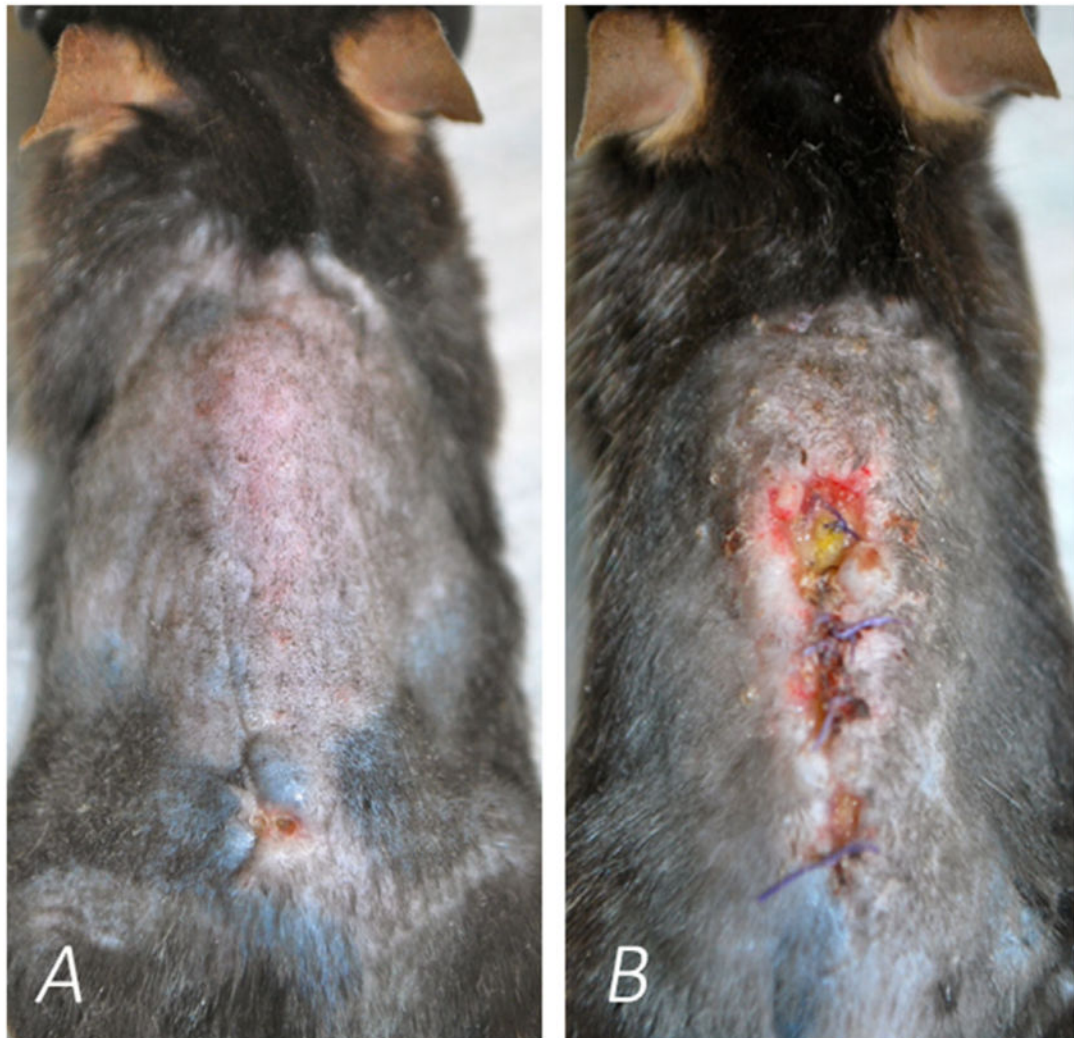


**Figure 4.** Images of the dorsal skin of mice inoculated with *S. aureus* Xen36 during a spine implant infection. (A) Mouse inoculated with  $1 \times 10^3$  CFUs, and intact dorsal skin (B) Mouse inoculated with  $1 \times 10^4$  CFUs, and evidence of considerable wound breakdown.

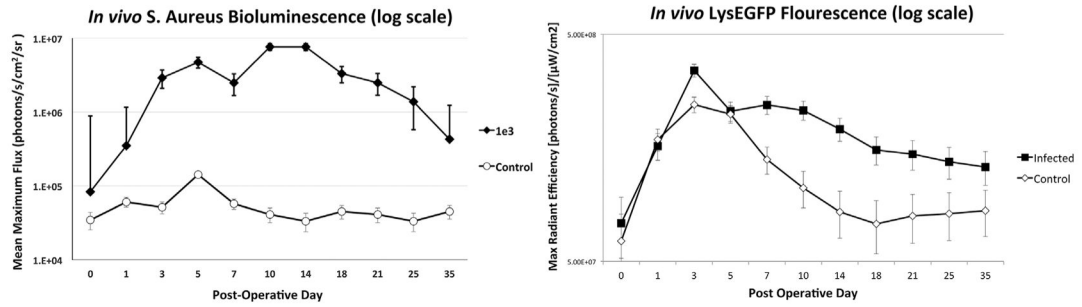


**Figure 5.**

In vivo bioluminescence and EGFP-neutrophil fluorescence induced by the Xen36 *S. aureus* strain during a spinal implant infection.  $1 \times 10^3$  CFUs of *S. aureus* a strain possessing the bioluminescent construct in a stable plasmid (Xen36) or a saline control ( $n=6$  mice per group) were inoculated into the L4 spinous process of mice in the presence of a stainless steel implant. (A) Bacterial counts as measured by in vivo *S. aureus* bioluminescence (mean maximum flux [photons/s/cm<sup>2</sup>/sr]  $\pm$  sem [logarithmic scale]). (B) Neutrophil infiltration (EGFP-neutrophil fluorescence) as measured by in vivo fluorescence (max radiant efficiency [(photons/s)/[ $\mu$ W/cm<sup>2</sup>)]  $\pm$  sem [logarithmic scale]).